Eur. Phys. J. D **33**, 213–220 (2005)
DOI: 10.1140/epjd/e2005-00039-3

THE EUROPEAN PHYSICAL JOURNAL D

Excitation-autoionization cross-sections and rate coefficients for Ge-like ions

P. Mandelbaum[1,2,a], M. Cohen[2], J.L. Schwob[2], and A. Bar-Shalom[3]

[1] Jerusalem College of Engineering, Ramat Beth Hakerem, 91035 Jerusalem, Israel
[2] Racah Institute of Physics, The Hebrew University, 91904 Jerusalem, Israel
[3] Nuclear Research Center-Negev, P.O. Box 9001, 84190 Beer Sheva, Israel

Received 7 December 2004
Published online 12 April 2005 –

Abstract. Results of cross-section and rate coefficient calculations for electron impact direct and indirect ionization of ions belonging to the GeI isoelectronic sequence (ground $3d^{10}4s^24p^2$) are presented. The cross-sections are given at near threshold energies for the five ions Kr^{4+}, Mo^{10+}, Xe^{22+}, Pr^{27+} and Dy^{34+}. The rate coefficients are computed for all the ions from Kr^{4+} to U^{60+} in the GeI sequence at seven electron temperatures ($kT_e = 0.1E_I, 0.3E_I, 0.5E_I, 0.7E_I, E_I, 2E_I$ and $10E_I$, where E_I is the first ionization energy). The calculations include the contribution of direct ionization (DI) calculated with the Lotz formula approximation and the contributions of excitation-autoionization (EA) calculated in the framework of the distorted wave (DW) approximation for the $4s - nl$, $3d - nl$ and $3p - nl$ resonant inner-shell excitations. The ionization enhancement due to the EA channels is shown as a function of Z along the GeI isoelectronic sequence.

PACS. 34.80.Kw Electron-ion scattering; excitation and ionization – 34.80.Dp Atomic excitation and ionization by electron impact

1 Introduction

Electron impact ionization is one of the important processes occurring in high temperature astrophysical and laboratory plasmas. Hot plasmas of highly ionized heavy elements are produced in magnetic and inertial confinement fusion and X-ray lasers experiments. Modeling the physics of these systems requires accurate calculations of cross-sections and rate coefficients for electron impact ionization in order to determine the ionization equilibrium and diagnose electron temperature and density. For ions with outer subshell having a high electron occupancy number, direct ionization (DI) as calculated from the parametrized Lotz formula is believed to predict quite well the total electron impact ionization cross-sections or rate coefficients. However, for ions with few outer electrons and an inner shell with a large occupancy number, indirect processes involving inner-shell excitation can become very important. Theoretical calculations have shown the importance of excitation-autoionization (EA) processes, in particular for ions of the NaI sequence (see for example [1]). These calculations reproduced very well experimental results when available. The importance of EA processes in other sequences was pointed out. In particular, it was shown by a study of the line emission in Ga-like rare earth ions emitted from Tokamak plasmas [2] that such processes could be very significant for ions of the GaI isoelectronic sequence. More generally, further calculations showed the ionization enhancement due to EA processes through $3d - 4l$ inner-shell excitation for ions in isoelectronic sequences with $3d^{10}4s^n4p^m$ ground configurations [3]. In the present paper one carries out extensive calculations of electron impact direct ionization and EA cross-sections and rate coefficients for ions along the GeI isoelectronic sequence (ground $3d^{10}4s^24p^2$). This work comes as a continuation of the previous works performed for the CuI (ground $3d^{10}4s$) [4], ZnI (ground $3d^{10}4s^2$) [5] and GaI (ground $3d^{10}4s^24p$) [6] isoelectronic sequences. In these previous works, it was shown that resonant $3l - 4l'$ electron impact excitations give a very significant EA contribution to the total ionization. For the GeI isoelectronic sequence, however, since the ground configuration has two electrons in the outer open $4p$ shell, the complexity of the calculations involved increases significantly. For five ions of this isoelectronic sequence (Kr^{4+}, Mo^{10+}, Xe^{22+}, Pr^{27+} and Dy^{34+}) the electron impact ionization cross-sections are presented as a function of the electron kinetic energy. The EA rate coefficients were computed for different electron temperatures for all the ions of the sequence. The EA calculations include $3d-nl$ ($n = 4$ to 8; $l = 0$ to 4) and $3p-nl$ ($n = 4$ and 5; $l = 0$ to 4) inner-shell electron impact excitations. For the lower members of the isoelectronic sequence (Kr^{4+} to Mo^{10+}) the contributions of the $4s-nl$ ($n = 5$ to 8; $l = 0$ to 4) excitations were also included.

[a] e-mail: pinchasm@jce.ac.il

2 Theoretical methods

The ground configuration $4p^2$ of the Ge-like ions include five levels. The electron impact EA cross-sections and rate coefficients from each of these five levels have been calculated. But, since in most cases the calculation results show no significant differences for the cross-sections or rate coefficients for these levels, only the results for EA cross-section and rate coefficient from the true ground level g ($4s^24p^2_{1/2}(J = 0)$) are reported in this work. Moreover one assumes that the only important collisional processes in the plasma are electron impact excitation and direct ionization from g. Other electron impact processes are neglected. In this approximation, the total cross-section for EA from g to any level k of the Ga-like ion through inner-shell excitation of the Ge-like ion to any intermediate autoionizing level j within a given configuration (or configuration complex) C is given by [4]:

$$\sigma_C^{EA} = \sum_{j\in C} \sigma_{gj}(E) \left[\frac{\sum_k A^a_{jk} + \sum_i A_{ji} B^a_i}{\sum_k A^a_{jk} + \sum_i A_{ji}} \right] = \sum_{j\in C} \sigma_{gj}(E) B^a_j \quad (1)$$

where $\sigma_{gj}(E)$ is the cross-section for electron-impact excitation from level g to the inner-shell excited level j as a function of the incident electron energy E. A^a_{jk} is the rate coefficient for autoionization from level j to a level k of the Ga-like ion. A_{ji} is the Einstein coefficient for spontaneous emission from level j to any lower-lying Ge-like level i. B^a_j is the *multiple* or *effective branching ratio for autoionization* from level j, defined by the bracket term. This term contains in turn the effective branching ratio B^a_i for further (secondary) autoionization from level i, defined by a similar recursive expression. This model allows one to take into account all the possible secondary autoionizations following cascading, until the ion reaches via radiative decay a level m below the first ionization limit ($B^a_m = 0$).

The present calculations have been performed using the *HULLAC* computer package [7]. This computer code gives full intermediate coupling energy level calculations including configuration interactions and Einstein radiative decay rate coefficients calculated in the framework of the central field approximation. The autoionization rate coefficients and the electron-impact collision strengths are calculated in the framework of the DW approximation. The cross-section $\sigma_{gj}(E)$ is related to the dimensionless symmetric collision strength $\Omega(i \rightarrow j)$ by:

$$\sigma_{ij}(E) = \frac{\pi a_0^2}{k_i^2 g_i} \Omega(i \rightarrow j) \quad (2)$$

where a_0 is the Bohr radius, $k_i^2 = E_i(Ry)[1 + \frac{\alpha^2}{4} E_i(Ry)]$ and $\alpha = e^2/\hbar c$. For plasma modeling studies, rate coefficients rather than cross-sections are used. The rate coefficient S_C^{EA} for excitation-autoionization from the level g of the ground configuration $3d^{10}4s^24p^2$ of a Ge-like ion to a level k of the Ga-like ion through inner-shell excitation to any intermediate autoionizing level j within the Ge-like configuration C as a function of the electron temperature T_e is given by:

$$S_C^{EA}(T_e) = \int_0^\infty \sigma_C^{EA} v f(v) dv = \sum_{j\in C} B^a_j Q_{gj}(T_e) \quad (3)$$

where v is the electron velocity and $f(v)$ is the electron velocity distribution (assumed Maxwellian). Q_{gj} is the electron-impact excitation rate coefficient from the ground level g to level j of the intermediate configuration. The total EA rate coefficients through the various intermediate autoionizing configurations

$$S^{EA} = \sum_C S_C^{EA} \quad (4)$$

were calculated for all the ions with $34 \leq Z \leq 92$ of the GeI isoelectronic sequence. The calculations were performed in the electron temperature range $0.1E_I \leq kT_e \leq 10E_I$, where E_I is the first ionization limit for each ion.

The EA contributions have been compared to the direct ionization cross-sections and rate coefficients calculated with the Lotz formula [8]. The cross-section $\sigma^{DI}(E)$ and the rate coefficient $S^{DI}(T_e)$ for direct electron impact ionization (including inner-shell direct ionization) of an ion in the ground state by electron impact are given according to the Lotz formula by:

$$\sigma^{DI}(E) = 4.5 \times 10^{-14} \sum_s \zeta_s \frac{\ln(E/E_s)}{E \times E_s} \quad (5)$$

$$S^{DI}(T_e) = 3.0 \times 10^{-6} \sum_s \frac{\zeta_s}{kT_e^{3/2}} \left[\frac{E_1(E_s/kT_e)}{(E_s/kT_e)} \right] \quad (6)$$

where $\sigma^{DI}(E)$ is given in cm^2 and S^{DI} in $cm^3\,s^{-1}$. E is the incident electron kinetic energy and kT_e is the electron temperature both in eV, ζ_s is the electron occupancy number of the s subshell, E_s is the binding energy in eV of the electrons in this subshell and E_1 is the exponential integral function. Table 1 gives the binding energies in eV for $4p(= E_I)$, $4s$, $3d$ and $3p$ electrons of the Ge-like ions in their ground state, calculated using the *HULLAC* code.

3 Contributions of EA processes

3.1 3d-nl inner-shell excitations

The first step in this work was to calculate the contributions of the $3d - nl$ electron impact inner-shell excitations to the EA processes. The calculations for these processes include excitations from the ground configuration $3d^{10}4s^24p^2$ of the Ge-like ion to the $3d^94s^24p^2nl$ ($4 \leq n \leq 8$; $0 \leq l \leq 4$) inner-shell autoionizing configurations. The $3d^94s4p^4$ configuration was also introduced for taking into account $sd - p^2$ configuration interaction. For the radiative transitions decays, all the relevant low-lying configurations are taken into account: the radiative transitions from the inner-shell excited configurations to the ground configuration ($nl \rightarrow 3d$ transition), radiative

Table 1. Binding energies (in eV) for $4p(= E_I)$, $4s$, $3d$ and $3p$ electrons for Ge-like ions.

Ion	$4p$	$4s$	$3d$	$3p$
Kr^{4+}	62.1	73.7	149.1	282.2
Rb^{5+}	82.8	96.1	188.2	318.0
Sr^{6+}	103.8	118.9	229.4	373.5
Y^{7+}	126.8	143.6	273.1	419.9
Zr^{8+}	152.1	170.8	320.8	476.9
Nb^{9+}	179.1	199.7	371.5	531.9
Mo^{10+}	207.5	230.0	424.7	596.9
Tc^{11+}	238.8	263.2	481.8	657.4
Ru^{12+}	271.3	297.7	541.9	724.4
Rh^{13+}	305.8	334.2	605.0	795.3
Pd^{14+}	341.9	372.3	670.9	871.1
Ag^{15+}	380.1	412.5	740.3	945.2
Cd^{16+}	420.2	454.7	812.0	1023
In^{17+}	461.8	498.5	887.2	1108
Sn^{18+}	505.6	544.4	965.3	1199
Sb^{19+}	551.2	592.1	1047	1286
Te^{20+}	598.9	642.0	1131	1379
I^{21+}	648.2	693.6	1219	1474
Xe^{22+}	699.4	747.0	1309	1572
Cs^{23+}	752.5	802.4	1401	1675
Ba^{24+}	807.8	859.9	1499	1776
La^{25+}	864.8	919.2	1598	1885
Ce^{26+}	923.8	980.5	1701	1994
Pr^{27+}	984.7	1044	1805	2111
Nd^{28+}	1048	1109	1915	2227
Pm^{29+}	1112	1176	2026	2348
Sm^{30+}	1180	1246	2139	2475
Eu^{31+}	1247	1316	2258	2598
Gd^{32+}	1319	1390	2379	2729
Tb^{33+}	1392	1466	2504	2862
Dy^{34+}	1467	1543	2629	3000
Ho^{35+}	1544	1623	2759	3140
Er^{36+}	1623	1704	2891	3282
Tm^{37+}	1705	1789	3028	3428
Yb^{38+}	1787	1873	3163	3579
Lu^{39+}	1874	1962	3307	3730
Hf^{40+}	1963	2054	3450	3885
Ta^{41+}	2052	2146	3599	4042
W^{42+}	2145	2241	3749	4208
Re^{43+}	2239	2338	3904	4374
Os^{44+}	2336	2437	4059	4538
Ir^{45+}	2434	2539	4220	4713
Pt^{46+}	2534	2642	4382	4883
Au^{47+}	2638	2748	4547	5067
Hg^{48+}	2745	2858	4716	5249
Tl^{49+}	2854	2969	4889	5433
Pb^{50+}	2964	3083	5063	5623
Bi^{51+}	3078	3199	5241	5813
Po^{52+}	3193	3318	5421	6010
At^{53+}	3311	3438	5605	6207
Rn^{54+}	3432	3562	5792	6413
Fr^{55+}	3554	3688	5978	6612
Ra^{56+}	3681	3818	6175	6827
Ac^{57+}	3810	3950	6371	7038
Th^{58+}	3941	4085	6570	7253
Pa^{59+}	4076	4223	6771	7473
U^{60+}	4213	4363	6975	8003

transitions to $3d^{10}4s^24pnl$ ($4 \le n \le 8$; $1 \le l \le 4$) through $4p \rightarrow 3d$ transition and also transitions among the levels of the considered inner-shell excited configurations ($nl \rightarrow nl'$ transition). The GaI-like configurations included in the second step of the EA processes are $3d^{10}4s^2nl$ ($n = 4$ and 5; $0 \le l \le 4$), $3d^{10}4s4p4l$ ($1 \le l \le 3$), $3d^{10}4s4d^2$ and $3d^{10}4p^3$. The model for the EA processes through the $3d-nl$ inner-shell excitation includes a total of 5082 levels.

3.2 3p-nl inner-shell excitations

For the EA contributions via $3p - nl$ electron impact excitations, the final model developed includes the ground configuration $3p^63d^{10}4s^24p^2$ of the Ge-like ion from which an electron can be excited to the $3p^53d^{10}4s^24p^2nl$ ($n = 4$, $1 \le l \le 3$; $n = 5$, $1 \le l \le 4$) inner-shell autoionizing configurations. Radiative decay is allowed among the levels of the above configurations and also to $3p^63d^{10}4s4p^2nl$ ($n = 4$, $1 \le l \le 3$; $n = 5$, $1 \le l \le 4$), through $4s \rightarrow 3p$ decay and to $3p^63d^94s^24p^2nl$ ($n = 4$, $1 \le l \le 3$; $n = 5$, $1 \le l \le 4$) through $3p \rightarrow 3d$ decay. The GaI-like configurations included are $3d^{10}4s^24l$ ($1 \le l \le 3$) and $3d^{10}4s4p^2$. The EA model for the $3p - nl$ inner-shell excitation includes 3057 levels.

3.3 4s-nl inner-shell excitations

For the lighter ions of the isoelectronic sequence, it was found that $4s - nl$ inner-shell excitations could give substantial contributions to the EA cross-sections. Thus, for the Kr^{4+} to Mo^{10+} ions a model for the $4s - nl$ excitation was created. This model includes the ground configuration $3p^63d^{10}4s^24p^2$ of the Ge-like ion from which an electron can be excited to the $3p^63d^{10}4s4p^2nl$ ($4 \le n \le 8$; $0 \le l \le 4$) inner-shell autoionizing configurations. Radiative decay is allowed among the levels of these configurations and also to $3p^63d^{10}4s^24pnl$ ($4 \le n \le 8$; $1 \le l \le 4$). The GaI-like configurations included are $3d^{10}4s^2nl$ ($4 \le n \le 6$; $1 \le l \le 4$) and $3d^{10}4s4p^2$. The EA model for the $4s - nl$ electron impact excitation includes 1323 levels.

4 Results

4.1 EA and direct ionization cross-sections

Table 2 displays the results of the present calculations for the electron impact DI and EA cross-section contributions for Kr^{4+}, Mo^{10+}, Xe^{22+}, Pr^{27+} and Dy^{34+} near the threshold energy.

Table 2. Computed electron impact ionization cross-sections near the threshold energy for Kr^{4+} (E_I = 62.1 eV), Mo^{10+} (E_I = 207.5 eV), Xe^{22+} (E_I = 699.4 eV), Pr^{27+} (E_I = 984.7 eV) and Dy^{34+} (E_I = 1467 eV). The first column gives the incident electron impact energy in eV. The next four columns give the direct ionization and the partial EA contribution of $4s-nl$, $3d-np$ and $3p-nl$ inner-shell excitations. All cross-sections are in cm^2 units.

(a) Kr^{4+}

E(eV)	Direct	$4s-nl$	$3d-nl$	$3p-nl$	E(eV)	Direct	$4s-nl$	$3d-nl$	$3p-nl$
65	1.70[−18]	2.03[−18]	0.0	0.0	105	1.02[−17]	6.21[−18]	2.01[−18]	0.0
70	2.61[−18]	5.31[−18]	0.0	0.0	110	1.08[−17]	5.92[−18]	2.43[−18]	0.0
75	3.52[−18]	7.28[−18]	0.0	0.0	115	1.12[−17]	5.66[−18]	3.29[−18]	0.0
80	4.72[−18]	7.62[−18]	0.0	0.0	120	1.14[−17]	5.43[−18]	4.48[−18]	0.0
85	5.92[−18]	7.76[−18]	1.84[−19]	0.0	125	1.16[−17]	5.22[−18]	5.17[−18]	0.0
90	7.12[−18]	7.30[−18]	2.11[−18]	0.0	130	1.17[−17]	5.04[−18]	5.34[−18]	0.0
95	8.32[−18]	6.89[−18]	2.17[−18]	0.0	135	1.18[−17]	4.87[−18]	6.52[−18]	0.0
100	9.52[−17]	6.53[−18]	2.06[−18]	0.0	140	1.18[−17]	4.71[−18]	7.01[−18]	0.0

(b) Mo^{10+}

E(eV)	Direct	$4s-nl$	$3d-nl$	$3p-nl$	E(eV)	Direct	$4s-nl$	$3d-nl$	$3p-nl$
210	2.47[−20]	1.90[−20]	0.0	0.0	290	6.15[−19]	7.02[−20]	1.40[−18]	0.0
220	1.15[−19]	7.19[−20]	2.10[−19]	0.0	300	6.82[−19]	6.74[−20]	1.35[−18]	0.0
230	1.94[−19]	9.53[−20]	2.50[−19]	0.0	310	7.42[−19]	6.48[−20]	1.55[−18]	0.0
240	2.63[−19]	8.99[−20]	2.40[−19]	0.0	320	7.96[−19]	6.25[−20]	2.29[−18]	0.0
250	3.23[−19]	8.46[−20]	2.45[−19]	0.0	330	8.44[−19]	6.04[−20]	2.25[−18]	0.0
260	3.76[−19]	8.07[−20]	3.78[−19]	0.0	340	8.88[−19]	5.86[−20]	2.32[−18]	0.0
270	4.55[−19]	7.67[−20]	6.82[−19]	0.0	350	9.26[−19]	5.68[−20]	2.46[−18]	0.0
280	5.40[−19]	7.34[−20]	8.15[−19]	0.0	360	9.61[−19]	5.51[−20]	2.83[−18]	0.0

(c) Xe^{22+}

E(eV)	Direct	$4s-nl$	$3d-nl$	$3p-nl$	E(eV)	Direct	$4s-nl$	$3d-nl$	$3p-nl$
700	1.58[−22]	0.0	9.77[−22]	0.0	860	5.07[−20]	0.0	4.87[−19]	0.0
720	5.19[−21]	0.0	3.30[−20]	0.0	880	5.60[−20]	0.0	4.77[−19]	5.80[−21]
740	9.81[−21]	0.0	5.84[−20]	0.0	900	6.10[−20]	0.0	4.68[−19]	5.99[−20]
760	1.68[−20]	0.0	2.04[−19]	0.0	920	6.56[−20]	0.0	4.62[−19]	5.89[−20]
780	2.47[−20]	0.0	1.99[−19]	0.0	940	6.99[−20]	0.0	4.55[−19]	5.77[−20]
800	3.19[−20]	0.0	2.01[−19]	0.0	960	7.39[−20]	0.0	4.63[−19]	6.07[−20]
820	3.87[−20]	0.0	2.97[−19]	0.0	980	7.77[−20]	0.0	4.91[−19]	6.82[−20]
840	4.49[−20]	0.0	4.96[−19]	0.0	1000	8.12[−20]	0.0	5.15[−19]	6.82[−20]

(d) Pr^{27+}

E(eV)	Direct	$4s-nl$	$3d-nl$	$3p-nl$	E(eV)	Direct	$4s-nl$	$3d-nl$	$3p-nl$
1000	1.41[−21]	0.0	7.79[−20]	0.0	1320	3.56[−20]	0.0	2.56[−19]	4.03[−20]
1040	4.80[−21]	0.0	9.22[−20]	0.0	1360	3.85[−20]	0.0	2.79[−19]	4.31[−20]
1080	1.06[−20]	0.0	1.41[−19]	0.0	1400	4.11[−20]	0.0	3.02[−19]	6.36[−20]
1120	1.59[−20]	0.0	2.73[−19]	0.0	1440	4.34[−20]	0.0	2.96[−19]	6.30[−20]
1160	2.08[−20]	0.0	2.66[−19]	3.71[−20]	1480	4.55[−20]	0.0	2.96[−19]	7.28[−20]
1200	2.51[−20]	0.0	2.58[−19]	3.61[−20]	1520	4.74[−20]	0.0	3.11[−19]	7.14[−20]
1240	2.90[−20]	0.0	2.52[−19]	3.52[−20]	1560	4.92[−20]	0.0	3.08[−19]	7.57[−20]
1280	3.25[−20]	0.0	2.47[−19]	4.07[−20]	1600	5.08[−20]	0.0	3.15[−19]	7.55[−20]

(e) Dy^{34+}

E(eV)	Direct	$4s-nl$	$3d-nl$	$3p-nl$	E(eV)	Direct	$4s-nl$	$3d-nl$	$3p-nl$
1500	8.75[−22]	0.0	2.18[−20]	0.0	1850	1.34[−20]	0.0	5.63[−20]	2.08[−20]
1550	2.34[−21]	0.0	6.26[−20]	0.0	1900	1.48[−20]	0.0	6.66[−20]	3.46[−20]
1600	4.68[−21]	0.0	6.11[−20]	1.99[−20]	1950	1.59[−20]	0.0	7.25[−20]	3.41[−20]
1650	6.69[−21]	0.0	5.96[−20]	1.99[−20]	2000	1.71[−20]	0.0	8.18[−20]	3.34[−20]
1700	8.63[−21]	0.0	5.81[−20]	1.95[−20]	2050	1.81[−20]	0.0	8.04[−20]	3.91[−20]
1750	1.04[−20]	0.0	5.68[−20]	2.13[−20]	2100	1.90[−20]	0.0	7.94[−20]	3.85[−20]
1800	1.19[−20]	0.0	5.60[−20]	2.10[−20]	2150	1.99[−20]	0.0	8.50[−20]	3.79[−20]

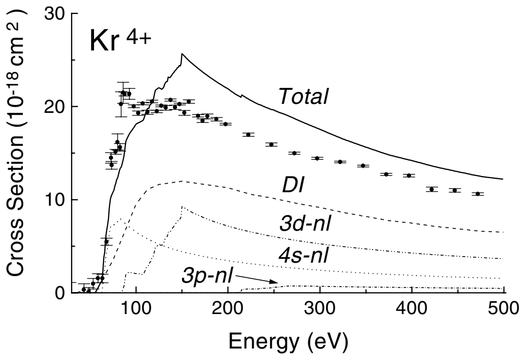

Fig. 1. Calculated direct-ionization cross-section (DI), $4s-nl$, $3d-nl$ and $3p-nl$ partial EA cross-sections, and total EA plus direct ionization cross-section as a function of the incident electron energy for the Kr^{4+} ion. The experimental results given by Bannister, Guo and Kojima [9] are also displayed.

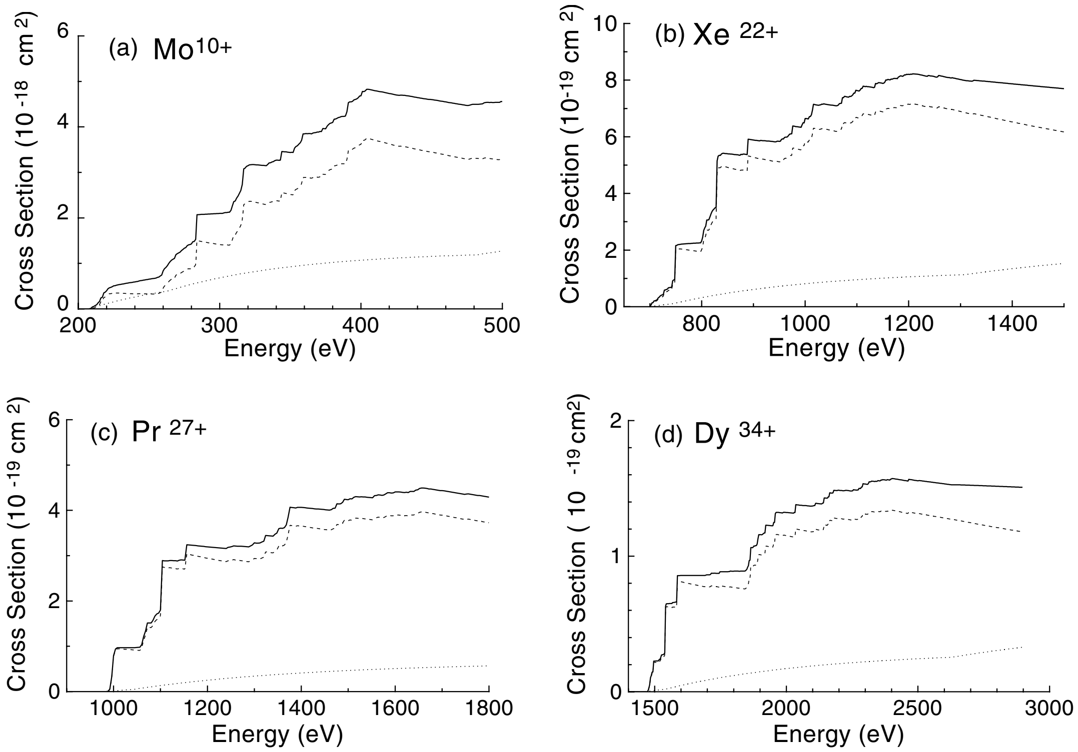

Fig. 2. Calculated direct-ionization cross-sections (dotted line), total EA cross-sections (dashed line), and total EA plus direct ionization cross-sections (solid line) as a function of the incident electron energy for the Mo^{10+}, Xe^{22+}, Pr^{27+} and Dy^{34+} ions.

The calculated EA cross-sections for Kr^{4+} together with the experimental results of Bannister et al. [9] are shown in Figure 1. The theoretical data for the direct ionization cross-section are from Gorczyca et al. [10]. At low electron impact energies $62.1 \leq E \leq 85$ eV the main EA contribution is from $4s-nl$ inner-shell excitation. For these low energies, the experimental data of Bannister et al. [9] are quite well reproduced. The underestimation of the theoretical curve in the 75 eV $\leq E \leq$ 90 eV energy range is probably due to the limitation of our $4s-nl$ EA calculations to n values below 9. The computed threshold for $3d-4p$ excitation is 85.6 eV and 100.2 eV for $3d-4d$. These are the main electron impact EA channels at the intermediate energies 85 eV $\leq E \leq$ 100 eV. At higher energies, there is an overestimation of the total cross-section of about 20% with respect to the experimental results. A very similar trend was observed with the computed cross-sections of Kr^{7+} in the CuI sequence [4] compared to the experimental results of Bannister et al. At our best knowledge, there are no published experimental data for the electron impact ionization cross-section for heavier ions of the GeI isoelectronic sequence. Thus for the higher Z elements of the sequence, no assessment of the computation accuracy could be made. Nevertheless, many previous works performed with the $HULLAC$ code have shown that the accuracy of the computations increases as a function of the ion charge Z. The main reason of this trend is the central field approximation on which the calculation of the electron wavefunction is based. This approximation is also better for high Z since correlation effects become negligible and relativistic effects that are very important for higher Z are fully taken into account.

Figures 2a to 2d display the results of the direct ionization and total EA cross-section computations for Mo^{10+}, Xe^{22+}, Pr^{27+} and Dy^{34+}. These are ions of the same elements for which cross-sections have been presented in the previous works for the CuI and ZnI isoelectronic sequences [4,5].

For Mo^{10+} (Tab. 2b and Fig. 2a) the $4s-nl$ EA channels are less important than for Kr^{4+}, since the inner-shell excited levels are autoionizing only for $n > 7$. The threshold for $3d-4p$ excitation is 213.5 eV, slightly above the ionization limit at 207.5 eV. This channel is the main EA channel in the low electron impact energy range 213.5 eV $\leq E \leq$ 257 eV. The onset of the $3d-4d$ EA channel is at 257 eV and $3p-4p$ at 381.5 eV.

The results for the EA cross-sections in Xe^{22+} are given in Table 2c and Figure 2b. For Xe^{22+} the contribution to EA of the $4s-nl$ excitation is negligible. The $3d^9 4s^2 4p^3$ configuration in Xe^{22+}, reached from the ground by $3d-4p$ excitation spans the 612−665 eV energy range, below the ionization energy ($E_I = 699.4$ eV). Thus the $3d-4d$ excitation turns to be the main EA channel at low electron impact energies ($E < 788$ eV). At higher energies ($800 < E < 870$ eV) the $3d-4f$ excitation is dominant, whereas the $3p-4p$ excited $3p^5 3d^{10} 4s^2 4p^3$ configuration spans the 875−976 eV energy range.

For Pr^{27+} (Tab. 2d and Fig. 2c) the $3d-4d$ excitation gives still the dominant EA contribution in the range near ionization-threshold (929−1062 eV), and the $3d-4f$ excitation in the intermediate 1057−1166 eV energy range.

Finally, in Dy^{34+} (Tab. 2e and Fig. 2d) both excitations: $3d-4d$ (1316−1511 eV) and $3d-4f$ (1474−1653 eV) give significant EA contributions near the ionization energy threshold ($E_I = 1467$ eV).

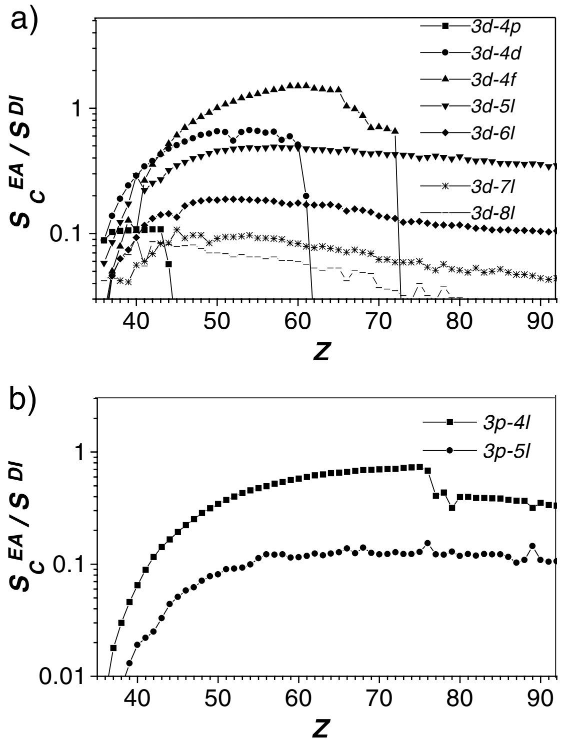

Fig. 3. Ratio of the excitation-autoionization rate coefficient S_C^{EA} to the direct ionization rate coefficient S^{DI} for (a) the $3d-nl$ and (b) the $3p-nl$ inner-shell excitations at electron temperature equal to the first ionization energy E_I, as a function of the atomic number Z, along the GeI isoelectronic sequence.

4.2 EA and direct ionization rate coefficients

The partial excitation-autoionization rate coefficients for the various ions in the GeI isoelectronic sequence were computed by detailed level-by-level calculations for $4s-nl$ (n = 4 to 8), $3d-nl$ (n = 4 to 8) and $3p-nl$ (n = 4 and 5) inner-shell excitations in a wide temperature range $0.1E_I \leq kT_e \leq 10E_I$. Table 3 gives the final results for the total ionization rate coefficient $S = S^{DI} + S^{EA}_{4s-nl} + S^{EA}_{3d-nl} + S^{EA}_{3p-nl}$ for all the Ge-like ions, from Kr^{4+} to U^{60+} at seven electron temperatures. The widely applied analytical Lotz formula has been used to compute the direct ionization rate S^{DI}.

Figures 3a and 3b show the ratios S_C^{EA}/S^{DI} for the $3d-nl$ ($n = 4$ to 8) and $3p-nl$ ($n = 4$ and 5) individual excitation channels respectively, calculated at $kT_e = E_I$ as a function of the Z number of the ion. This allows to compare the *relative* importance of the contributions from the various inner-shell excitation channels to the total ionization rate. From Figure 3a, one can see that the behavior of the contributions of the $3d-4l$ channels are very different from the quite regular behavior of the contributions of the higher $3d-nl$ ($n \geq 5$) channels. For ions having $Z \leq 44$ there is a contribution of $3d-4p$ excitations. But for ions with $Z \geq 45$, the $3d-4p$ inner-shell excited levels lie below the first ionization limit, thus the $3d-4p$ contribution falls abruptly. The same phenomenon occurs with the $3d-4d$ channel and with the dominant $3d-4f$ channel at $Z = 63$ and $Z = 74$, respectively. The contributions of the $3p-4l$ channels (Fig. 3b) show a similar pattern. For $Z = 75$ the contribution of the $3p-4l$ excitations begins to decrease as some of the $3p-4d$ inner-shell excited levels lie below the ionization limit. But most of the $3p-4f$ inner-shell excited levels (as the $3p-5l$ excited configurations) remain above the ionization limit for the rest of the isoelectronic sequence, contributing significantly to the total ionization rate coefficient.

Figure 4 displays the ionization enhancement factor due to all the EA processes $R^{EA} = (S^{DI} + S^{EA}_{Total})/S^{DI}$ for three temperatures $kT_e = 0.1E_I, 0.5E_I$ and E_I. The results of the present calculations show that the total EA contribution is very significant. At $kT_e = 0.1E_I$, R^{EA} reaches a maximum of about 16 for $Nd^{28+}(Z = 60)$. At $kT_e = 0.5E_I$, R^{EA} shows still a maximum of 7 for this ion. This last value must be compared with a maximum of about 10 calculated for $Z = 43$ in the CuI isoelectronic sequence (Fig. 9 in Ref. [4]), and for $Z = 55$ in the ZnI isoelectronic sequence (Fig. 8 in Ref. [5]). As expected, the relative importance of the EA versus DI processes decreases as the number of electrons in the outer shell is larger. But on the other side, as predicted in reference [3], for the isoelectronic sequences with a larger number of outer electrons, the $3d-4l$ inner-shell excited configurations remain autoionizing for larger Z elements. Thus, if one considers for example, the Sm^{33+} (Cu-like), Sm^{32+} (Zn-like) and Sm^{30+} (Ge-like) ions ($Z = 62$),

Table 3. Computed total DI plus EA ionization rate coefficients S at seven electron temperatures for all the Ge-like ions, from Kr^{4+} to U^{60+}. The electron temperature is given in terms of the first ionization energy E_I given in Table 1. The rate coefficients are given in $cm^3\,s^{-1}$ units. $X[-Y]$ means $X \times 10^{-Y}$.

Ion	$kT_e = 0.1E_I$	$0.3E_I$	$0.5E_I$	$0.7E_I$	E_I	$2E_I$	$10E_I$
Kr^{4+}	4.89[–13]	5.70[–10]	2.56[–9]	5.06[–9]	8.70[–9]	1.71[–8]	2.93[–8]
Rb^{5+}	3.27[–13]	3.87[–10]	1.81[–9]	3.66[–9]	6.36[–9]	1.27[–8]	2.14[–8]
Sr^{6+}	2.51[–13]	2.96[–10]	1.41[–9]	2.87[–9]	5.02[–9]	9.95[–9]	1.66[–8]
Y^{7+}	1.50[–13]	2.15[–10]	1.09[–9]	2.28[–9]	4.03[–9]	8.00[–9]	1.33[–8]
Zr^{8+}	1.19[–13]	1.84[–10]	9.49[–10]	1.98[–9]	3.48[–9]	6.80[–9]	1.10[–8]
Nb^{9+}	9.67[–14]	1.60[–10]	8.21[–10]	1.70[–9]	2.95[–9]	5.71[–9]	9.13[–9]
Mo^{10+}	7.00[–14]	1.38[–10]	7.26[–10]	1.51[–9]	2.62[–9]	4.99[–9]	7.85[–9]
Tc^{11+}	7.04[–14]	1.32[–10]	6.73[–10]	1.37[–9]	2.35[–9]	4.39[–9]	6.76[–9]
Ru^{12+}	5.68[–14]	1.20[–10]	6.10[–10]	1.23[–9]	2.09[–9]	3.88[–9]	5.87[–9]
Rh^{13+}	4.82[–14]	1.11[–10]	5.55[–10]	1.11[–9]	1.88[–9]	3.43[–9]	5.11[–9]
Pd^{14+}	4.70[–14]	1.06[–10]	5.18[–10]	1.03[–9]	1.71[–9]	3.08[–9]	4.52[–9]
Ag^{15+}	4.87[–14]	1.01[–10]	4.84[–10]	9.49[–10]	1.57[–9]	2.77[–9]	4.02[–9]
Cd^{16+}	5.09[–14]	9.72[–11]	4.55[–10]	8.78[–10]	1.44[–9]	2.51[–9]	3.60[–9]
In^{17+}	5.24[–14]	9.18[–11]	4.20[–10]	8.05[–10]	1.30[–9]	2.25[–9]	3.20[–9]
Sn^{18+}	5.43[–14]	8.80[–11]	3.94[–10]	7.47[–10]	1.20[–9]	2.05[–9]	2.88[–9]
Sb^{19+}	5.50[–14]	8.33[–11]	3.66[–10]	6.87[–10]	1.10[–9]	1.86[–9]	2.59[–9]
Te^{20+}	5.67[–14]	7.94[–11]	3.42[–10]	6.36[–10]	1.01[–9]	1.70[–9]	2.34[–9]
I^{21+}	5.78[–14]	7.53[–11]	3.19[–10]	5.87[–10]	9.25[–10]	1.55[–9]	2.12[–9]
Xe^{22+}	5.86[–14]	7.13[–11]	2.97[–10]	5.44[–10]	8.51[–10]	1.42[–9]	1.93[–9]
Cs^{23+}	5.62[–14]	6.64[–11]	2.74[–10]	5.00[–10]	7.79[–10]	1.29[–9]	1.75[–9]
Ba^{24+}	5.70[–14]	6.29[–11]	2.55[–10]	4.61[–10]	7.16[–10]	1.18[–9]	1.60[–9]
La^{25+}	5.66[–14]	5.89[–11]	2.37[–10]	4.27[–10]	6.61[–10]	9.52[–10]	1.46[–9]
Ce^{26+}	6.32[–14]	5.63[–11]	2.23[–10]	3.98[–10]	6.13[–10]	9.99[–10]	1.34[–9]
Pr^{27+}	5.67[–14]	5.33[–11]	2.08[–10]	3.70[–10]	5.66[–10]	9.15[–10]	1.22[–9]
Nd^{28+}	5.70[–14]	5.01[–11]	1.93[–10]	3.42[–10]	5.22[–10]	8.42[–10]	1.12[–9]
Pm^{29+}	3.93[–14]	3.94[–11]	1.57[–10]	2.82[–10]	4.37[–10]	7.22[–10]	9.92[–10]
Sm^{30+}	3.05[–14]	3.30[–11]	1.34[–10]	2.43[–10]	3.79[–10]	6.34[–10]	8.81[–10]
Eu^{31+}	2.98[–14]	3.08[–11]	1.23[–10]	2.23[–10]	3.48[–10]	5.81[–10]	8.11[–10]
Gd^{32+}	2.93[–14]	2.88[–11]	1.14[–10]	2.07[–10]	3.21[–10]	5.38[–10]	7.43[–10]
Tb^{33+}	2.91[–14]	2.71[–11]	1.07[–10]	1.92[–10]	2.97[–10]	4.96[–10]	6.88[–10]
Dy^{34+}	2.48[–14]	2.27[–11]	8.98[–11]	1.62[–10]	2.52[–10]	4.23[–10]	5.90[–10]
Ho^{35+}	2.39[–14]	2.10[–11]	8.26[–11]	1.49[–10]	2.32[–10]	3.89[–10]	5.43[–10]
Er^{36+}	2.03[–14]	1.84[–11]	7.35[–11]	1.34[–10]	2.10[–10]	3.56[–10]	5.04[–10]
Tm^{37+}	1.71[–14]	1.59[–11]	6.42[–11]	1.17[–10]	1.85[–10]	3.14[–10]	4.48[–10]
Yb^{38+}	1.78[–14]	1.53[–11]	4.44[–11]	1.10[–10]	1.73[–10]	2.94[–10]	4.17[–10]
Lu^{39+}	1.67[–14]	1.27[–11]	5.61[–11]	1.02[–10]	1.10[–10]	2.72[–10]	3.87[–10]
Hf^{40+}	1.61[–14]	1.33[–11]	5.23[–11]	9.49[–11]	1.49[–10]	2.53[–10]	3.60[–10]
Ta^{41+}	2.18[–15]	8.61[–12]	3.65[–11]	6.87[–11]	1.11[–10]	1.96[–10]	2.87[–10]
W^{42+}	7.74[–15]	8.18[–12]	3.45[–11]	6.45[–11]	1.04[–10]	1.83[–10]	2.69[–10]
Re^{43+}	7.66[–15]	7.81[–12]	3.27[–11]	6.11[–11]	9.84[–11]	1.73[–10]	2.52[–10]
Os^{44+}	3.09[–15]	5.96[–12]	2.80[–11]	5.48[–11]	9.15[–11]	1.69[–10]	2.26[–10]
Ir^{45+}	2.88[–15]	5.09[–12]	2.33[–11]	4.53[–11]	7.54[–11]	1.39[–10]	2.12[–10]
Pt^{46+}	2.86[–15]	4.94[–12]	2.25[–11]	4.37[–11]	7.25[–11]	1.33[–10]	2.02[–10]
Au^{47+}	2.72[–15]	4.60[–12]	2.09[–11]	4.16[–11]	6.72[–11]	1.23[–10]	1.89[–10]
Hg^{48+}	2.64[–15]	4.36[–12]	1.97[–11]	3.82[–11]	6.34[–11]	1.16[–10]	1.78[–10]
Tl^{49+}	2.58[–15]	4.13[–12]	1.28[–11]	3.58[–11]	5.94[–11]	1.09[–10]	1.67[–10]

Table 3. *Continued.*

Ion	$kT_e = 0.1E_I$	$0.3E_I$	$0.5E_I$	$0.7E_I$	E_I	$2E_I$	$10E_I$
Pb^{50+}	2.51[–15]	3.90[–12]	1.75[–11]	3.38[–11]	5.60[–11]	1.03[–10]	1.57[–10]
Bi^{51+}	2.49[–15]	3.74[–12]	1.67[–11]	3.18[–11]	5.31[–11]	9.75[–11]	1.50[–10]
Po^{52+}	2.44[–15]	3.56[–12]	1.58[–11]	3.03[–11]	5.02[–11]	9.18[–11]	1.41[–10]
At^{53+}	2.40[–15]	3.40[–12]	1.50[–11]	2.88[–11]	4.75[–11]	8.71[–11]	1.33[–10]
Rn^{54+}	2.32[–15]	3.21[–12]	1.41[–11]	2.71[–11]	4.47[–11]	8.19[–11]	1.26[–10]
Fr^{55+}	2.27[–15]	3.04[–12]	1.33[–11]	2.56[–11]	4.22[–11]	7.75[–11]	1.19[–10]
Ra^{56+}	2.23[–15]	2.93[–12]	1.28[–11]	2.45[–11]	4.03[–11]	7.38[–11]	1.14[–10]
Ac^{57+}	2.21[–15]	2.80[–12]	1.22[–11]	2.32[–11]	3.82[–11]	7.00[–11]	1.08[–10]
Th^{58+}	2.16[–15]	2.68[–12]	1.16[–11]	2.21[–11]	3.65[–11]	6.68[–11]	1.03[–10]
Pa^{59+}	2.06[–15]	2.51[–12]	1.09[–11]	2.08[–11]	3.43[–11]	6.29[–11]	9.72[–11]
U^{60+}	2.01[–15]	2.38[–12]	1.03[–11]	1.95[–11]	3.22[–11]	5.91[–11]	9.15[–11]

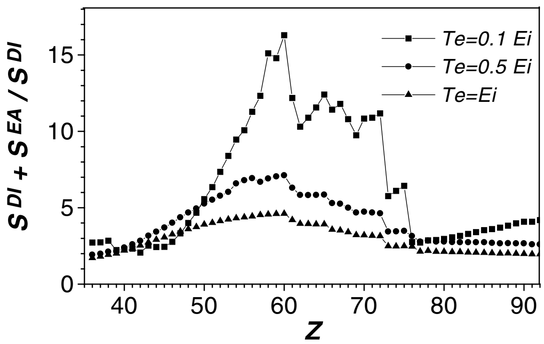

Fig. 4. Ionization enhancement factor due to EA at three electron temperature $kT_e = 0.1E_I, 0.5E_I$ and E_I as a function of the atomic number Z, along the GeI isoelectronic sequence.

the calculated enhancement factors R^{EA} are 4.2, 5.5 and 5.8 respectively (at $kT_e = 0.5E_I$), in contrast to the previous mentioned usual trend. This is due here to the fact that the $3d-4l$ inner-shell excitations do not contribute to EA processes in Sm^{33+} and Sm^{32+} (since the excited configurations are below the ionization potential), but give the most important contribution to EA in Sm^{30+}.

5 Conclusion

In the present work, detailed DW calculations for EA processes along the GeI isoelectronic sequence have been performed. The computed ionization cross-sections are presented for five ions for energies near the ionization threshold. The total ionization rate coefficients for all the ions from Kr^{4+} to U^{60+} in the ground level have been calculated. The calculations include the direct ionization obtained from the Lotz formula and the EA contributions for $4s-nl$ ($n=4$ to 8), $3d-nl$ ($n=4$ to 8) and $3p-nl$ ($n=4$ and 5) inner-shell excitations calculated with the $HULLAC$ code in the framework of the DW approximation. These calculations show the very important role of the EA channels, even for isoelectronic sequences with several electrons in the outer shell.

References

1. D.L. Moores, K.J. Reed, Adv. At. Mol. Opt. Phys. **34**, 301 (1995)
2. P. Mandelbaum et al., Phys. Rev. A **42**, 4412 (1990)
3. D. Mitnik, P. Mandelbaum, J.L. Schwob, A. Bar-Shalom, J. Oreg, W.H. Goldstein, Phys. Rev. A **50**, 4911 (1994)
4. D. Mitnik, P. Mandelbaum, J.L. Schwob, A. Bar-Shalom, J. Oreg, W.H. Goldstein, Phys. Rev. A **53**, 3178 (1996)
5. D. Mitnik, P. Mandelbaum, J.L. Schwob, A. Bar-Shalom, J. Oreg, Phys. Rev. A **55**, 307 (1997)
6. J. Oreg, W. Goldstein, P. Mandelbaum, D. Mitnik, E. Meroz, J.L. Schwob, A. Bar-Shalom, Phys. Rev. A **44**, 1741 (1991)
7. A. Bar-Shalom, M. Klapisch, J. Oreg, J. Quant. Spec. Rad. Transfer **71**, 169 (2001)
8. W. Lotz, Z. Phys. **206**, 205 (1967); W. Lotz, Z. Phys. **216**, 241 (1968)
9. M.E. Bannister, X.Q. Guo, T.M. Kojima, Phys. Rev. A **49**, 4676 (1994)
10. T.W. Gorczyca, M.S. Pindzola, N.R. Badnell, D.C. Griffin, Phys. Rev. A **49**, 4682 (1994)